Mol. Cells 2014; 37(5): 399-405
http://dx.doi.org/10.14348/molcells.2014.0042

Molecules and Cells
http://molcells.org
Established in 1990

A Revised Assay for Monitoring Autophagic Flux in *Arabidopsis thaliana* Reveals Involvement of *AUTOPHAGY-RELATED9* in Autophagy

Kwang Deok Shin, Han Nim Lee, and Taijoon Chung*

Autophagy targets cytoplasmic cargo to a lytic compartment for degradation. Autophagy-related (Atg) proteins, including the transmembrane protein Atg9, are involved in different steps of autophagy in yeast and mammalian cells. Functional classification of core Atg proteins in plants has not been clearly confirmed, partly because of the limited availability of reliable assays for monitoring autophagic flux. By using *proUBQ10-GFP-ATG8a* as an autophagic marker, we showed that autophagic flux is reduced but not completely compromised in *Arabidopsis thaliana atg9* mutants. In contrast, we confirmed full inhibition of autophagic flux in *atg7* and that the difference in autophagy was consistent with the differences in mutant phenotypes such as hypersensitivity to nutrient stress and selective autophagy. Autophagic flux is also reduced by an inhibitor of phosphatidylinositol kinase. Our data indicated that *atg9* is phenotypically distinct from *atg7* and *atg2* in *Arabidopsis,* and we proposed that ATG9 and phosphatidylinositol kinase activity contribute to efficient autophagy in *Arabidopsis*.

INTRODUCTION

In diverse eukaryotic species, autophagy targets a portion of the cytoplasm to a lytic compartment for bulk degradation (Yang and Klionsky, 2010). The best-characterized type of autophagy is macroautophagy (hereinafter referred to as autophagy), which is initiated by the formation of a membrane cisterna called the phagophore. A phagophore is an expanded membrane sac that sequesters cytoplasmic constituents and matures into the autophagosome, a double-membraned cytoplasmic compartment. In yeast and plant cells, the outer membrane of the autophagosome fuses with the vacuolar membrane. In the vacuole, the inner membrane and its cargo are called an autophagic body, which is rapidly degraded by vacuolar hydrolases.

A set of *Autophagy-related* (*Atg*) genes is responsible for autophagy in yeast and is conserved in higher eukaryotes. Homology-based reverse genetic studies have revealed the function of autophagy in plants (Li and Vierstra, 2012). On the basis of the classification of conserved yeast and mammalian *Atg* genes involved in phagophore initiation and expansion (Yang and Klionsky, 2010), it was proposed that core ATG homologs in *Arabidopsis* are classified into four groups (Kim et al., 2012): (i) ATG1 kinase complex containing ATG13 (Suttangkakul et al., 2011) and ATG11 (Li et al., 2014); (ii) phosphatidylinositol (PI) 3-kinase complex containing VPS34 and ATG6 (Liu et al., 2005); generating phosphatidylinositol 3-phosphate (PI3P), which may be enriched in autophagic membrane (Zhang et al., 2011); (iii) ATG8 and ATG12 conjugation system containing ATG7 (Doelling et al., 2002), ATG4 (Yoshimoto et al., 2004), ATG5 (Thompson et al., 2005), ATG10 (Phillips et al., 2008), and ATG12 (Chung et al., 2010); and (iv) transmembrane protein ATG9 (Hanaoka et al., 2002; Inoue et al., 2006) and ATG2-ATG18a complex (Inoue et al., 2006; Xiong et al., 2005). All *Arabidopsis* mutants defective in ATG8 and ATG12 conjugation showed the same degree of phenotype (Chung et al., 2010). For example, *atg7, atg5, atg10, atg4a atg4b* double, and *atg12a atg12b* double mutants were unable to survive 12 days of darkness, while more than 50% of wild-type seedlings were still recovered after the dark treatment (Chung et al., 2010). During post-germinative growth, *atg5* and *atg7* mutant hypocotyls also showed similar stabilization of peroxisomal proteins (Kim et al., 2013). However, only a few studies have revealed phenotypic differences among multiple classes of *Arabidopsis atg* mutants (Hofius et al., 2009; Inoue et al., 2006; Suttangkakul et al., 2011; Wang et al., 2011).

Yeast Atg9 and its mammalian homolog ATG9 are thought to act early in autophagosome formation, but detailed mode of action may differ between two homologues (Zavodszky et al., 2013). Yeast Atg9 is required for autophagy (Noda et al., 2000), whereas mammalian ATG9 appears to be important but not strictly required for this process (Orsi et al., 2012). Yeast Atg9 interacts with Atg2 and with PI3P-binding Atg18 (Wang et al., 2001), all of which are localized at the edge of the phagophore (Suzuki et al., 2013). In fact, recent studies suggested that *Atg1, Atg2,* and *Atg18* are all interconnected and regulate Atg9 traf

Department of Biological Sciences, Pusan National University, Busan 609-735, Korea
*Correspondence: taijoon@pusan.ac.kr

Received 25 February, 2014; revised 30 March, 2014; accepted 8 April, 2014; published online 7 May, 2014

Keywords: concanamycin A, GFP-ATG8 processing assay, pexophagy, plant autophagy, wortmannin

eISSN: 0219-1032

fickin in yeast (Zavodszky et al., 2013). In contrast, interactions of mammalian ATG9 with ATG2 and ATG18 were not reported, and the relation between ATG9 and ATG2-ATG18 remains unclear.

Arabidopsis *atg9-1* was described as the first plant *atg* mutant (Hanaoka et al., 2002), although it is not clear whether this mutant is deficient for autophagy. Wild type (WT) and mutants homozygous for the second allele, *atg9-2*, accumulated cytoplasmic inclusions in the vacuole when they were treated with protease inhibitors (Inoue et al., 2006). In contrast, *atg2* and *atg5* mutants accumulated much less cytoplasmic inclusions in the vacuole, suggesting that autophagy in *Arabidopsis* roots requires *ATG2* and *ATG5* but not *ATG9* (Inoue et al., 2006). Thus, it appears that *Arabidopsis ATG9* and *ATG2* belong to different classes of core *ATG* genes. To confirm the functional classification of *Arabidopsis ATG* genes, further information must be obtained from comparative analysis of *atg* mutants, which must be validated by assays for autophagy (Klionsky et al., 2012). However, the dispensability of *ATG9* for autophagy in *Arabidopsis* was not confirmed by analysis with the autophagic marker GFP-ATG8, which was used to demonstrate that autophagy is inhibited in *atg7* (Chung et al., 2010), *atg5* (Chung et al., 2010), and *atg2* (Wang et al., 2011).

Autophagic flux is defined as the dynamic process of autophagosome synthesis, delivery of autophagic substrates to the lytic compartment, and degradation of autophagic substrates inside the lytic compartment (Mizushima et al., 2010). Determination of autophagic flux is important because a steady-state level of autophagic markers may be increased not only by induction of autophagy but also by a block in a later step such as fusion or vacuolar degradation (Klionsky et al., 2012). Concanamycin A (CA), an inhibitor of vacuolar proton pumps (Matsuoka et al., 1997), is useful for monitoring autophagic flux in plants. Treatment with CA leads to increased vacuolar pH and inactivation of acid hydrolases in the vacuole. The objective of this study was to identify phenotypic difference between *atg7, atg9,* and *atg2* mutants. By using autophagic markers and inhibitors, we found that *atg9* mutants are phenotypically distinct from *atg7* and *atg2* and exhibited reduced autophagic flux when compared to WT.

MATERIALS AND METHODS

Plant materials and growth conditions

TAIR Accession numbers of *Arabidopsis* genes mentioned are as follows: ATG2, AT3G19190; ATG5, AT5G17290; ATG7, AT5G45900; ATG8a, AT4G21980; ATG9, AT2G31260. *Arabidopsis thaliana* T-DNA insertional mutants *atg2-1* (Inoue et al., 2006), *atg5-1* (Thompson et al., 2005), *atg7-2* (Chung et al., 2010), *atg9-3* (SALK_128991), and *atg9-4* (SALK_145980) were previously described or obtained from the Arabidopsis Information Resource (TAIR, http://arabidopsis.org). Transgenic marker lines expressing *GFP-ATG8a* under the control of the cauliflower mosaic virus *35S* promoter (Thompson et al., 2005) and *Arabidopsis UBQ10* promoter (Kim et al., 2013) were designated *pro35S-GFP-ATG8a* and *proUBQ10-GFP-ATG8a*, respectively.

Surface-sterilized *Arabidopsis* seeds were stored at 4°C for 3 days and incubated at 20-22°C under a 16-h light/8-h dark photoperiod. For liquid culture, seedlings were incubated in a 24-well plate containing Murashige-Skoog (MS) liquid medium supplemented with 1% (w/v) sucrose (Kim et al., 2013). Nitrogen supply to the seedlings was limited by changing the medium to liquid MS-N containing 1% sucrose (Chung et al., 2009). For solid culture, seeds were germinated on MS solid medium with 1% sucrose (Kim et al., 2013). A carbon starvation experiment was performed as described previously (Chung et al., 2010).

Immunoblot analysis

Seeds were germinated on the solid medium for analysis of isocitrate lyase; hydroponically grown seedlings were used for all other analyses. Dissected hypocotyls (for isocitrate lyase; Ettinger and Harada, 1990) or whole seedlings (other analysis) were homogenized in Laemmli buffer and clarified by centrifugation at 16,000 × *g* for 10 min. Protein samples were separated by 12% SDS-PAGE. Immunoblot analysis was performed as described previously (Kim et al., 2013) except that anti-GFP antibodies (Roche) were diluted to 1:2000.

Microscopy

Nine-day-old root tissues from the maturation zone were analyzed using a Zeiss 510 laser scanning confocal microscope (Carl Zeiss). GFP was excited with a 488-nm excitation line and a BP500-530IR emission filter was used for detection. Z-sections through the central vacuole were acquired at 1-μm intervals to distinguish autophagic bodies from transvacuolar strands.

RESULTS

ATG9 is not strictly essential for autophagy but affects autophagic flux

To investigate the requirement of *ATG9* for autophagy in *Arabidopsis*, we used two *atg9* alleles, designated *atg9-3* and *atg9-4*. The *atg9-3* and *atg9-4* alleles have a T-DNA insertion in exon 6 and in the 5′ end of exon 8, respectively, of the single-copy *ATG9* gene (Supplementary Fig. S1). Reverse transcriptase (RT)-PCR analysis detected no *ATG9* transcript flanking the T-DNA insertion in *atg9-3* and *atg9-4*, indicating that they are null for functional *ATG9* transcripts (Supplementary Fig. S1D).

We initially crossed the *atg9* mutants with transgenic plants carrying the *pro35S-GFP-ATG8a* transgene (Thompson et al., 2005), a popular marker for the autophagosome and autophagic bodies. However, we observed a marked reduction in GFP signal in the progeny produced from the crosses, compared to GFP from the original *pro35S-GFP-ATG8a* transgenic line (data not shown). The reduction likely resulted from transgene silencing, because the presence of cauliflower mosaic virus *35S* promoter in T-DNA tagging mutants often represses transgene expression driven by the same promoter (Daxinger et al., 2008). Thus, we decided to use an alternative marker, *proUBQ10-GFP-ATG8a* (Kim et al., 2013), which contains the promoter of Arabidopsis *UBQ10* gene instead of the *35S* promoter. We crossed the *proUBQ10-GFP-ATG8a* transgenic plants with *atg9-3* and *atg9-4*, and their F_2 individuals were genotyped to obtain *atg9* mutants containing the transgene. The *proUBQ10-GFP-ATG8a* seedlings with WT, *atg7-2, atg9-3,* or *atg9-4* background were incubated in liquid medium containing either CA or dimethylsulfoxide (DMSO) as a solvent control. CA is frequently used to stabilize vacuolar GFP-ATG8a puncta, which are interpreted as autophagic bodies (Yoshimoto et al., 2004). Confocal microscopy of DMSO-treated WT and *atg9* roots (Fig. 1A) revealed a diffuse GFP-ATG8a signal in the cytoplasm, except for the occasional puncta that may show phagophores or autophagosomes. The CA-treated WT vacuole contained numerous GFP-ATG8a-labeled autophagic bodies, while the *atg7-2* vacuole did not contain GFP-ATG8a puncta,

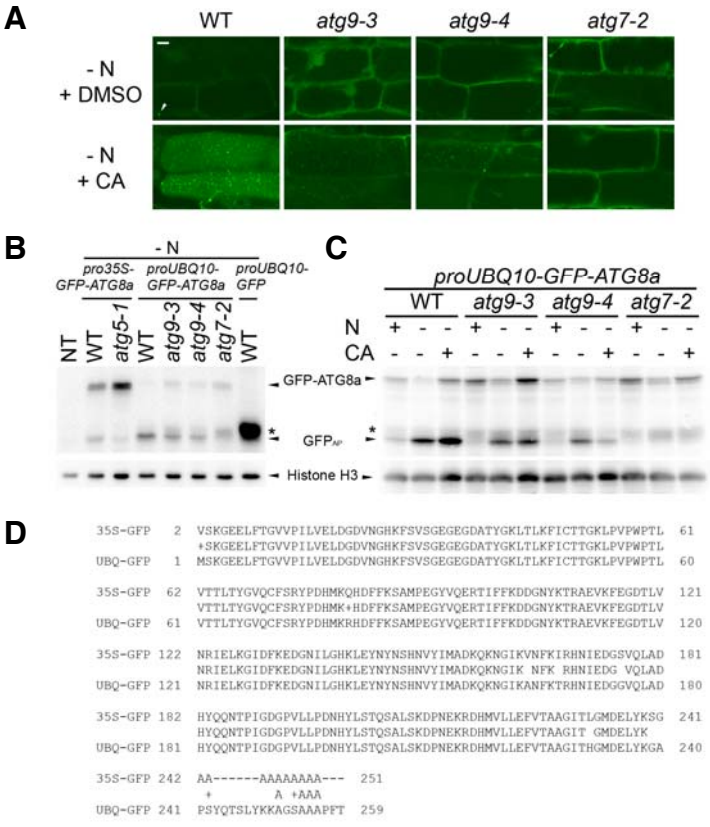

Fig. 1. Autophagic marker analysis of *atg7-2* and *atg9* mutants. Hydroponically grown 7-d-old *Arabidopsis* seedlings were further incubated in either nitrogen (N)-sufficient or -deficient medium for 2 days before analysis. (A) Subcellular localization of GFP-ATG8a in N-limited wild-type (WT), *atg9-3, atg9-4,* and *atg7-2* roots. Eight-day-old *proUBQ10-GFP-ATG8a* seedlings with indicated genotypes were treated with either 1 μM concanamycin A (CA, second row) or an equal volume of dimethylsulfoxide (DMSO, first row) for 16 h, and analyzed by confocal microscopy. Arrowhead shows a phagophore-like signal. Representative images were chosen from at least five biological replicates. Scale bar = 10 μm. (B) and (C) GFP-ATG8 processing assay of *atg9* and *atg7* mutants. Non-transgenic WT (NT), *pro35S-GFP-ATG8a, proUBQ10-GFP*, and *proUBQ10-GFP-ATG8a* transgenic seedlings of indicated genotypes were incubated in N-sufficient liquid medium for 7 days and then incubated in N-deficient medium for 2 days before immunoblot analysis (B). In (C), N-supplied or -limited seedlings were treated with CA (+) or DMSO (-) for 16 h prior to protein extraction. Immunoblot analysis by using anti-GFP (upper panel) or anti-histone H3 (lower panel; loading control) antibodies was performed. Arrowheads show the protein bands corresponding to GFP-ATG8a, GFP_{AP}, and histone H3. Asterisk indicates the position of protein bands corresponding to GFP_{IP} which shows slightly slower mobility than that by GFP_{AP}. Representative immunoblots were selected from at least three independent experiments. (D) Comparison of two autophagic marker lines, *pro35S-GFP-ATG8a* (upper lines, 35S-GFP) and *proUBQ10-GFP-ATG8a* (lower lines, UBQ-GFP), by pairwise alignment of N-terminal amino acid sequences that were predicted from *GFP-ATG8a* coding sequences in two transgenic constructs.

as previously reported (Chung et al., 2010). GFP-ATG8a puncta were detected in the vacuole of CA-treated *atg9* seedlings, although they were not as abundant as in the WT (Fig. 1A).

To monitor autophagic flux in *atg9* seedlings, we carried out the GFP-ATG8 processing assay (Klionsky et al., 2012). This assay is routinely used to study autophagy in yeast and is based on the fact that GFP-ATG8 in the vacuole is processed to generate free GFP which is more stable than GFP-ATG8. Autophagy-deficient mutants typically lack free GFP, whereas the inhibition of vacuolar degradation results in accumulation of free GFP and GFP-ATG8. Although the assay can be used for plant cells (Chung et al., 2010; Suttangkakul et al., 2011), there is a potential problem with this method. In *atg5-1* mutants expressing the conventional autophagic marker *pro35S-GFP-ATG8a* (Thompson et al., 2005), we often detected a faint protein band (Fig. 1B, lane 3) that co-migrated with the free GFP band in the WT extract (Fig. 1B, lane 2). Interestingly, when we used *proUBQ10-GFP-ATG8a* for anti-GFP immunoblot analysis (Figs. 1B and 1C), we identified three protein bands with different mobility in SDS-PAGE: one band at the predicted size of GFP-ATG8a, and two faster bands similar to the size of free GFP moiety. The WT had the fastest band, *atg7-2* had a smear band with slightly slower mobility (indicated by asterisks in Figs. 1B and 1C), and *atg9-3* and *atg9-4* included both. In the WT, the intensity of the fastest protein band was increased by nitrogen limitation and further by CA treatment. These increases suggest that this band represents a processed GFP species that is more stable than GFP-ATG8a in the vacuole and is thus a true indicator of autophagic flux. This protein species was designated GFP_{AP} (for *a*utophagy-dependent, *p*rocessed GFP). In contrast, the slower band appeared to be associated with inefficient autophagy, as it was rarely detectable in the WT but more noticeable in *atg9-3, atg9-4,* and *atg7-2*; this protein species was designated GFP_{IP} (for autophagy-*i*ndependent, *p*rocessed GFP). Although GFP_{IP} level was slightly increased by nitrogen limitation in *atg7* and *atg9* mutants, it was not increased by CA (Fig. 1C, smear bands indicated by asterisk), showing that GFP_{IP} is not associated with the vacuole and cannot be considered an indicator of autophagic flux.

Compared to WT, *atg9* seedlings contained a lower level of GFP_{AP} (Figs. 1B and 1C), indicating reduced autophagic flux in the mutants. The *atg9* mutants showed a WT-like increase in GFP_{AP} in response to nitrogen limitation, but unlike the WT, CA treatment had only a minor effect on GFP_{AP} levels in these mutants (Fig. 1C). Since CA mainly acts after the fusion of the autophagosome with the vacuole, this result suggested that *ATG9* acts in an early step before the fusion event.

We further tested the hypothesis that GFP_{AP} is a product of vacuolar degradation. Tamura et al. (2003) reported that GFP tagged with a C-terminal vacuolar-targeting signal is processed in the vacuole, and that a processed GFP moiety was stabilized when plants were incubated in the dark. Consistent with our hypothesis, the abundance of GFP_{AP}, but not of GFP_{IP}, was increased when *proUBQ10p-GFP-ATG8a* plants were incubated in the dark (Fig. 2).

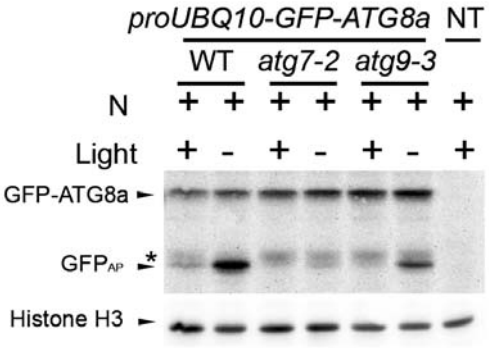

Fig. 2. Response of autophagic marker lines to light deprivation. Autophagic marker lines *proUBQ10-GFP-ATG8a* with indicated genotypes were incubated in N-sufficient liquid medium for 8 days. At day 8, a plate containing the seedlings was wrapped with aluminum foil (- light) and another plate was left illuminated (+ light). After 24 h, proteins were extracted from the seedlings and immunoblot analysis was performed using anti-GFP (upper panel) or anti-histone H3 (lower panel, loading control) antibodies. Arrowheads show the protein bands corresponding to GFP-ATG8a, GFP_{AP}, and histone H3. Asterisk indicates the position of protein bands corresponding to GFP_{IP} which shows slightly slower mobility than that by GFP_{AP}. NT, non-transgenic control.

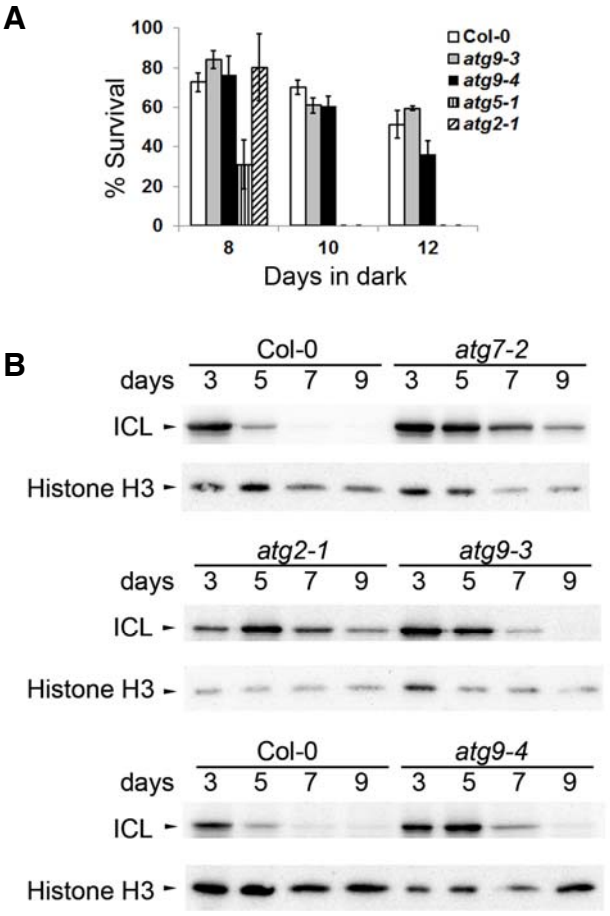

Fig. 3. Phenotypes of *atg7-2*, *atg2-1*, and *atg9* mutants. (A) Carbon starvation phenotype was assessed using a light-deprivation experiment (Chung et al., 2010). Two-week-old seedlings were deprived of light for the indicated number of days. Percentage of survival was calculated from self-fertilized progenies collected from ≥ 4 parental plants. Mean ± S.E. (N = 4 or 5 sibling populations) (B) Peroxisomal protein degradation in hypocotyls of the indicated genotypes was assessed by immunoblot analysis using anti-isocitrate lyase (ICL, upper panels) and anti-histone H3 (lower panels; loading control) antibodies. Representative immunoblots were selected from at least three independent experiments.

Phenotypes of *atg9* differ from those of *atg7* and *atg2*

We compared *atg7, atg2,* and *atg9* for hypersensitivity to nutrient limitation, which is the canonical phenotype of autophagy-defective *Arabidopsis* mutants (Doelling et al., 2002; Hanaoka et al., 2002; Inoue et al., 2006). As expected from our analysis of autophagy, *atg7-2* and *atg2-1* showed hypersensitivity to fixed carbon limitation (Chung et al., 2010), but *atg9* seedlings did not (Fig. 3A). Phenotypic differences between *atg9* and other core *atg* mutants were also seen for phenotypes associated with pexophagy, a selective type of autophagy preferentially targeting peroxisomes for degradation (Kim et al., 2013). Degradation of isocitrate lyase (ICL), a peroxisomal matrix enzyme, was shown to be delayed in *atg7* and *atg5* hypocotyls (Kim et al., 2013). Delayed degradation was also confirmed in *atg2*-1 hypocotyls (Fig. 3B), consistent with a recent report that another *atg2* allele suppressed defects in peroxisomal functions (Farmer et al., 2013). ICL degradation was also delayed in *atg9* hypocotyls (Fig. 3B), although *atg7-2* and *atg2-1* contained a higher level of ICL at day 9 than *atg9* did. These phenotypic data were consistent with our observation that autophagic flux was fully compromised in *atg7* and *atg2* but not in *atg9*.

Wortmannin blocks autophagic flux

To determine whether PI 3-kinase activity is required for autophagy in plant cells, we tested the effect of wortmannin (WM), an inhibitor of mammalian and plant PI 3-kinases (Matsuoka et al., 1995). We incubated *pro35S-GFP-ATG8a* transgenic seedlings in liquid medium containing CA for various durations; the effect of CA on the level of free GFP was prominent after 16 h of incubation (Supplementary Fig. S2A). Next, we incubated the transgenic plants in liquid medium containing either DMSO or CA and various amounts of WM for 16 h and found that 10-30 μM WM dampened the effect of CA on free GFP (Supplementary Figs. S2B and S2C). However, only a slight reduction in free GFP was seen in transgenic seedlings treated with 30 μM WM alone for 16 h, compared to DMSO control (Supplementary Fig. S2B) and no treatment control at 0 h (Supplementary Fig. S2D). These results suggested that PI 3-kinase activity is required for either vacuolar targeting of GFP-ATG8a or for stabilization of free GFP by CA.

To gain insight into the relationship between different core ATG complexes in plants, we further investigated the effects of CA and WM on the autophagic markers in various mutant backgrounds. We compared confocal images of *proUBQ10-GFP-ATG8a* transgenic roots of WT, *atg7-2, atg9-3,* and *atg9-4* background that were treated with DMSO, CA, WM, or the combination of CA and WM (Fig. 4A). The effect of CA in WT and *atg9* was markedly diminished by treatment with WM, indicating that efficient delivery of GFP-ATG8a to the vacuole relies on PI 3-kinase activity. In WM-treated WT and *atg9* cells, most

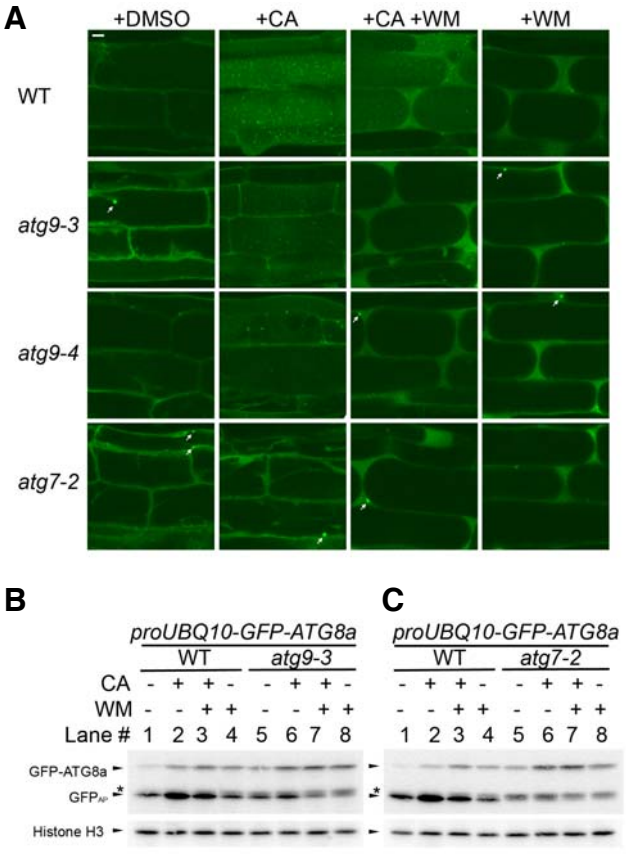

Fig. 4. Autophagic flux is blocked using wortmannin (WM). Nitrogen supply was limited to seedlings for 2 days prior to analysis. (A) Confocal microscopy of GFP-ATG8a transgenic roots treated with dimethylsulfoxide (DMSO), concanamycin A (CA), WM, or both. GFP-ATG8a transgenic roots from wild-type (WT, first row), *atg9-3* (second row), *atg9-4* (third row), and *atg7-2* (fourth row; negative control) background. Eight-day-old seedlings were further incubated for 16 h in liquid medium containing DMSO (first column), 1 μM CA (second column), 1 μM CA and 30 μM WM (third column), or 30 μM WM (fourth column). Representative images were chosen from at least five biological replicates. Scale bar = 10 μm. (B, C) Immunoblot analysis of GFP-ATG8a transgenic seedlings of WT, *atg9-3*, or *atg7-2* treated with DMSO, WM, CA, or WM and CA, as in (A). Immunoblots were reacted with anti-GFP (upper panels) or with anti-histone H3 (lower panels; loading control) antibodies. Arrowheads identify the protein bands corresponding to GFP-ATG8a, GFP_{AP}, and histone H3. Asterisk indicates the position of GFP_{IP}. A minus (-) sign represents no treatment, while a plus (+) sign means treatment with CA or WM. Representative immunoblots were selected from at least three independent experiments.

GFP-ATG8a signal appeared to be diffuse in the cytosol and to occasionally form cytoplasmic foci, but almost no signal was detected in *atg9* vacuoles. No GFP-ATG8a puncta were detected in the vacuoles of autophagy-defective negative control *atg7-2* treated with CA and WM.

We also investigated the effect of WM on autophagic flux. The GFP-ATG8 processing assay was performed using crude extracts prepared from whole seedlings that were treated with DMSO, CA, WM, or combination of CA and WM (Figs. 4B and 4C). We not only confirmed the absence of GFP_{AP} in *atg7-2* (Fig. 4C, lanes 5-8) and the presence of both GFP_{AP} and GFP_{IP} in *atg9* (Fig. 4B, lanes 5-7), but also observed a small amount of GFP_{IP} in WM-treated WT samples (Figs. 4B and 4C; lanes 3 and 4), suggesting that WM blocked a step in autophagy. In the WT, WM treatment increased the level of GFP-ATG8a but not that of GFP_{AP} (Figs. 4B and 4C; lanes 1 and 4), while CA treatment enhanced the intensity of both GFP-ATG8a and GFP_{AP} (Figs. 4B and 4C; lanes 1 and 2). WM treatment also suppressed the effect of CA on GFP_{AP} accumulation (Figs. 4B, C; lanes 2 and 3). Combined with the confocal microscopy data, these immunoblot data indicated that WM interferes with the targeting of cytoplasmic GFP-ATG8a-PE to the vacuole for processing to GFP_{AP} and then full degradation. GFP_{AP} was largely depleted in *atg9-3* seedlings by WM treatment alone (Fig. 4B, lanes 5 and 8), although CA stabilized a trace amount of GFP_{AP} (Fig. 4B, lanes 7 and 8). The additional inhibition by WM in *atg9* is consistent with the notion that ATG9 belongs to a different class from the autophagy-specific PI 3-kinase complex in *Arabidopsis*. In conclusion, the collective data confirmed that WM-sensitive PI 3-kinase activity and *ATG9* contribute to efficient autophagic flux, especially in early autophagic process prior to the fusion of the autophagosome with the vacuole (Fig. 4).

DISCUSSION

In this study, we compared different classes of core ATG proteins in *Arabidopsis*, by using genetic analysis, confocal microscopy, and the GFP-ATG8a processing assay. Our data confirmed that mutations affecting the ATG8 conjugation system and ATG2-ATG18 complex resulted in more severe phenotypes than did *atg9* (Figs. 1-4). ATG9 and PI 3-kinase activity may act at different stages of *Arabidopsis* autophagy, since *atg9* mutants retained sensitivity to WM (Fig. 4).

We developed an *Arabidopsis* GFP-ATG8 processing assay that can separate autophagy-dependent and -independent pools of free GFP processed from GFP-ATG8a. The former pool, named GFP_{AP}, which appeared to accumulate in the vacuole, was stabilized by CA and increased in response to N limitation. Thus, GFP_{AP} is an indicator of autophagic flux. The nature of the autophagy-independent pool (GFP_{IP}) is not clear, but GFP_{IP} may be related to reduction or blockage in autophagic flux. This speculation is based on our observation of GFP_{IP} in *atg7* and *atg9* seedlings (Figs. 1B, 1C, 2, 4B, and 4C).

Although the *pro35S-GFP-ATG8a* transgene (Thompson et al., 2005) has been popular as an autophagic marker in *Arabidopsis*, there are drawbacks to its use. We crossed the *pro35S-GFP-ATG8a* transgenic line with *atg9* mutants to obtain *atg9* mutants expressing the transgene but later found that the transgene was silenced in mutant progeny, probably because of the presence of the *35S* promoter (Daxinger et al., 2008). We used an alternative autophagic marker line, *proUBQ10-GFP-ATG8a* (Kim et al., 2013), in which GFP-ATG8a showed a lower level of accumulation (Fig. 1B). The calculated molecular weight of free GFP moieties predicted from *pro35S-GFP-ATG8a* and *proUBQ10-GFP-ATG8a,* were 27.8 and 28.9 kDa, respectively. The 1.1-kDa difference is mostly caused by the C-terminal residues of the GFP moiety, where the *pro35S-GFP-ATG8a* transgene has a polyalanine linker and the *proUBQ10-GFP-ATG8a* transgene has a different linker derived from a recombination site in the vector system (Fig. 1D). The explanation for why only *proUBQ10-GFP-ATG8a* resulted in the separation of GFP_{AP} from GFP_{IP} may lie in the differential C-terminal sequences. For example, the polyalanine linker may cause a

structurally weak junction (amino acids 242 to 251 of upper sequence in Fig. 1D) that is susceptible to attack by extravacuolar proteolytic activity, which may also attack at amino acids 254 to 256 of GFP-ATG8a derived from *proUBQ-GFP-ATG8a* (Fig. 1D, lower sequence) and generate a slightly longer GFP moiety, that is, GFP_{IP}. Only in autophagy-competent plants, GFP_{AP} may form by further digestion to ~240th amino acid by vacuolar proteases.

The difference in mobility between GFP_{AP} and GFP_{IP} is small. Thus, when the *proUBQ10-GFP-ATG8a* line is used for the GFP-ATG8 processing assay, it is recommended that protein samples be run with a reference sample (e.g., *atg9* or WM-treated WT extract) in SDS-PAGE. In addition, CA may be useful for confirming normal autophagic flux, as recommended previously (Klionsky et al., 2012). For example, we detected reduced autophagic flux in *atg9* that would not have been revealed without CA treatment (Figs. 1C and 4B).

Although WM and CA are useful as inhibitors of early and late steps in autophagy, respectively, it is important that they be used with caution. Since CA indirectly blocks the action of vacuolar hydrolases by inhibiting vacuolar proton pumps, it took 16 h of CA treatment for autophagic cargo to be markedly stabilized (Supplementary Fig. S2A). In addition, we treated *Arabidopsis* seedlings with liquid medium containing CA and WM-uptake efficiency by plant tissues is variable under such conditions (e.g., shoot tissues may be less affected by CA and WM than root tissues). This partial uptake may explain our observation that GFP_{AP} is only slightly increased by treatment of WT with CA and WM (Figs. 1 and 4) but significantly increased by dark treatment (Fig. 2).

We showed that *Arabidopsis ATG9* is not strictly required for autophagy but contributes to efficient autophagic flux and that *atg9* phenotypes are distinct from those of *atg2* and *atg7*. Our observation is consistent with that in previous studies of the *atg9-2* allele (Inoue et al., 2006) but contrasts with that in an earlier study of the *atg9-1* allele (Hanaoka et al., 2002). The *atg9-1* allele has a Wassilewskija genetic background, while *atg9-2, atg9-3,* and *atg9-4* alleles have a Columbia background. In addition, *atg9-1* has a large deletion spanning exons 4-10 near its T-DNA insertion (see Supplementary Fig. S1A). Hypersensitivity to carbon limitation was observed in *atg9-1* mutants (Hanaoka et al., 2002), while we did not note a marked difference from the WT (Fig. 3). We do not know the cause of this phenotypic difference; the difference may suggest that the C-terminal half of ATG9 is dispensable for its function if a partial ATG9 is produced from *atg9-2, atg9-3*, and *atg9-4* (see Supplementary Fig. S1A). Alternatively, variation in genetic background may explain the phenotypic differences among mutants. Analysis of autophagic flux in *atg9-1* will provide valuable information to help clarify this issue.

Note: Supplementary information is available on the Molecules and Cells website (www.molcells.org).

ACKNOWLEDGMENTS

We thank John Harada for kindly providing the anti-ICL antisera. This study was supported by the Basic Science Research Program through the National Research Foundation of Korea funded by the Ministry of Science, ICT and Future Planning (2011-0010683) and by a grant from the Next-Generation BioGreen 21 Program (No. PJ009004), Rural Development Administration, Republic of Korea.

REFERENCES

Chung, T., Suttangkakul, A., and Vierstra, R.D. (2009). The ATG autophagic conjugation system in maize: ATG transcripts and abundance of the ATG8-lipid adduct are regulated by development and nutrient availability. Plant Physiol. *149,* 220-234.

Chung, T., Phillips, A.R., and Vierstra, R.D. (2010). ATG8 lipidation and ATG8-mediated autophagy in *Arabidopsis* require ATG12 expressed from the differentially controlled ATG12A AND ATG12B loci. Plant J. *62,* 483-493.

Daxinger, L., Hunter, B., Sheikh, M., Jauvion, V., Gasciolli, V., Vaucheret, H., Matzke, M., and Furner, I. (2008). Unexpected silencing effects from T-DNA tags in *Arabidopsis*. Trends Plant Sci. *13,* 4-6.

Doelling, J.H., Walker, J.M., Friedman, E.M., Thompson, A.R., and Vierstra, R.D. (2002). The APG8/12-activating enzyme APG7 is required for proper nutrient recycling and senescence in *Arabidopsis thaliana*. J. Biol. Chem. *277,* 33105-33114.

Ettinger, W.F., and Harada, J.J. (1990). Translational or post-translational processes affect differentially the accumulation of isocitrate lyase and malate synthase proteins and enzyme activities in embryos and seedlings of *Brassica napus*. Arch. Biochem. Biophys. *281,* 139-143.

Farmer, L.M., Rinaldi, M.A., Young, P.G., Danan, C.H., Burkhart, S.E., and Bartel, B. (2013). Disrupting autophagy restores peroxisome function to an *Arabidopsis lon2* mutant and reveals a role for the LON2 protease in peroxisomal matrix protein degradation. Plant Cell *25,* 4085-4100.

Hanaoka, H., Noda, T., Shirano, Y., Kato, T., Hayashi, H., Shibata, D., Tabata, S., and Ohsumi, Y. (2002). Leaf senescence and starvation-induced chlorosis are accelerated by the disruption of an *Arabidopsis* autophagy gene. Plant Physiol. *129,* 1181-1193.

Hofius, D., Schultz-Larsen, T., Joensen, J., Tsitsigiannis, D.I., Petersen, N.H., Mattsson, O., Jorgensen, L.B., Jones, J.D., Mundy, J., and Petersen, M. (2009). Autophagic components contribute to hypersensitive cell death in *Arabidopsis*. Cell *137,* 773-783.

Inoue, Y., Suzuki, T., Hattori, M., Yoshimoto, K., Ohsumi, Y., and Moriyasu, Y. (2006). AtATG genes, homologs of yeast autophagy genes, are involved in constitutive autophagy in *Arabidopsis* root tip cells. Plant Cell Physiol. *47,* 1641-1652.

Kim, S.H., Kwon, C., Lee, J.H., and Chung, T. (2012). Genes for plant autophagy: functions and interactions. Mol. Cells *34,* 413-423.

Kim, J., Lee, H., Lee, H.N., Kim, S.H., Shin, K.D., and Chung, T. (2013). Autophagy-related proteins are required for degradation of peroxisomes in *Arabidopsis* hypocotyls during seedling growth. Plant Cell *25,* 4956-4966.

Klionsky, D.J., Abdalla, F.C., Abeliovich, H., Abraham, R.T., Acevedo-Arozena, A., Adeli, K., Agholme, L., Agnello, M., Agostinis, P., Aguirre-Ghiso, J.A., et al. (2012). Guidelines for the use and interpretation of assays for monitoring autophagy. Autophagy *8,* 445-544.

Li, F., and Vierstra, R.D. (2012). Autophagy: a multifaceted intracellular system for bulk and selective recycling. Trends Plant Sci. *17,* 526-537.

Li, F., Chung, T., and and Vierstra, R.D. (2014). AUTOPHAGY-RELATED (ATG)11 plays a critical role in general autophagy and senescence-induced mitophagy in *Arabidopsis*. Plant Cell *26,* 788-807.

Liu, Y., Schiff, M., Czymmek, K., Talloczy, Z., Levine, B., and Dinesh-Kumar, S.P. (2005). Autophagy regulates programmed cell death during the plant innate immune response. Cell *121,* 567-577.

Matsuoka, K., Bassham, D.C., Raikhel, N.V., and Nakamura, K. (1995). Different sensitivity to wortmannin of two vacuolar sorting signals indicates the presence of distinct sorting machineries in tobacco cells. J. Cell Biol. *130,* 1307-1318.

Matsuoka, K., Higuchi, T., Maeshima, M., and Nakamura, K. (1997). A vacuolar-type H^+-ATPase in a nonvacuolar organelle is required for the sorting of soluble vacuolar protein precursors in tobacco cells. Plant Cell *9,* 533-546.

Mizushima, N., Yoshimori, T., and Levine, B. (2010). Methods in mammalian autophagy research. Cell *140,* 313-326.

Noda, T., Kim, J., Huang, W.P., Baba, M., Tokunaga, C., Ohsumi, Y., and Klionsky, D.J. (2000). Apg9p/Cvt7p is an integral mem-

brane protein required for transport vesicle formation in the Cvt and autophagy pathways. J. Cell Biol. *148,* 465-480.
Orsi, A., Razi, M., Dooley, H.C., Robinson, D., Weston, A.E., Collinson, L.M., and Tooze, S.A. (2012). Dynamic and transient interactions of Atg9 with autophagosomes, but not membrane integration, are required for autophagy. Mol. Biol. Cell *23,* 1860-1873.
Phillips, A.R., Suttangkakul, A., and Vierstra, R.D. (2008). The ATG12-conjugating enzyme ATG10 Is essential for autophagic vesicle formation in *Arabidopsis thaliana*. Genetics *178,* 1339-1353.
Suttangkakul, A., Li, F., Chung, T., and Vierstra, R.D. (2011). The ATG1/ATG13 protein kinase complex is both a regulator and a target of autophagic recycling in *Arabidopsis*. Plant Cell *23,* 3761-3779.
Suzuki, K., Akioka, M., Kondo-Kakuta, C., Yamamoto, H., and Ohsumi, Y. (2013). Fine mapping of autophagy-related proteins during autophagosome formation in *Saccharomyces cerevisiae*. J. Cell Sci. *126,* 2534-2544.
Tamura, K., Shimada, T., Ono, E., Tanaka, Y., Nagatani, A., Higashi, S.I., Watanabe, M., Nishimura, M., and Hara-Nishimura, I. (2003). Why green fluorescent fusion proteins have not been observed in the vacuoles of higher plants. Plant J. *35,* 545-555.
Thompson, A.R., Doelling, J.H., Suttangkakul, A., and Vierstra, R.D. (2005). Autophagic nutrient recycling in *Arabidopsis* directed by the ATG8 and ATG12 conjugation pathways. Plant Physiol. *138,* 2097-2110.
Wang, C.W., Kim, J., Huang, W.P., Abeliovich, H., Stromhaug, P.E., Dunn, W.A., Jr, and Klionsky, D.J. (2001). Apg2 is a novel protein required for the cytoplasm to vacuole targeting, autophagy, and pexophagy pathways. J. Biol. Chem. *276,* 30442-30451.
Wang, Y., Nishimura, M.T., Zhao, T., and Tang, D. (2011). ATG2, an autophagy-related protein, negatively affects powdery mildew resistance and mildew-induced cell death in *Arabidopsis*. Plant J. *68,* 74-87.
Xiong, Y., Contento, A.L., and Bassham, D.C. (2005). AtATG18a is required for the formation of autophagosomes during nutrient stress and senescence in *Arabidopsis thaliana*. Plant J. *42,* 535-546.
Yang, Z., and Klionsky, D.J. (2010). Mammalian autophagy: core molecular machinery and signaling regulation. Curr. Opin. Cell Biol. *22,* 124-131.
Yoshimoto, K., Hanaoka, H., Sato, S., Kato, T., Tabata, S., Noda, T., and Ohsumi, Y. (2004). Processing of ATG8s, ubiquitin-like proteins, and their deconjugation by ATG4s are essential for plant autophagy. Plant Cell *16,* 2967-2983.
Zavodszky, E., Vicinanza, M., and Rubinsztein, D.C. (2013). Biology and trafficking of ATG9 and ATG16L1, two proteins that regulate autophagosome formation. FEBS Lett. *587,* 1988-1996.
Zhang, Y., Li, S., Zhou, L.Z., Fox, E., Pao, J., Sun, W., Zhou, C., and McCormick, S. (2011). Overexpression of *Arabidopsis thaliana* PTEN caused accumulation of autophagic bodies in pollen tubes by disrupting phosphatidylinositol 3-phosphate dynamics. Plant J. *68,* 1081-1092.